# Electrochemistry of copper( II) -peptide complexes containing histidine residues

**Kô Takehara*** and **Yasushi Ide**

*Laboratory of Chemistry, College of General Education, Kyushu University, Ropponmatsu, Chuo-ku, Fukuoka 810 (Japan)*

(Received September 3, 1990; revised December 5, 1990)

## Abstract

Copper( II) -peptide complexes (peptide = GHL**, GHG and GH) were investigated in aqueous solution by various electrochemical methods. The electrode reaction was measured at various pH levels. The distribution profile of the species was determined using potentiometric titration. After considering the effect of electrostatic repulsion between charged electrode surface and GHL, the coordination structure of Cu(II) -GHL determined by the two methods was in agreement. Electroplating was used to investigate the adsorption mechanism of Cu(II) -GHL, and it was found that the adsorption of Cu(II) -GHL changed the coordination structure of Cu(II) -GHL, causing a shift in the reduction potential of adsorbed Cu(II) -GHL toward the reduction potential of free Cu(II) ion.

## Introduction

Small peptides containing the histidine residue have been considered with interest as models of the metal ion binding site of bioactive peptides and proteins. Lau *et al.* studied the Cu( II) -GGH complex as a model of a copper ion binding site of human serum albumin [1, 2]. Yokoyama and coworkers reported the structures of coordination compounds of several transition metal ions with GGH, GHG and GH [3, 4]. Pickart and Thaler [5] first isolated GHL from human plasma and studied the various abilities in biological functions [6]. However there have been some conflicts on the assignment of coordination sites of GHL to copper ion [7-9].

Although many authors have reported on the coordination structures of metal peptide complexes based on potentiometric titration, there are few reports based on electrochemical behavior. Among them, Youngblood and Margerum studied the cyclic voltammetric behaviors of the Cu(II) -GGG complex and the ternary Cu(II) -GGG-( 2,9-dimethyl-1,10-phenanthroline) complex [10]. Zacharias and coworkers [11] and Bilewicz [12] reported the generation of Cu( I) species as intermediates in the reduction of Cu(II) -peptide complexes in the presence of excess amounts of peptide. Aihara *et al.* reported the effect of solvents on the reduction potentials of Cu( II) -dipeptide water/organic mixed solvents [13].

In the present paper, the coordination structures and the reaction mechanisms of Cu(II) -GHL are discussed in light of the results of potentiometric and electrochemical measurements. The adsorption mechanism of Cu(II) -GHL on the mercury electrode is also discussed.

## Experimental

### *Materials*

GHL was purchased from Peptide Institute Inc. GHG and GH were purchased from Sigma Chemicals. Potassium hydroxide used for potentiometry was a Merck Titrisol product. All other inorganic chemicals used were of analytical reagent grade. All peptides and inorganic chemicals were used without further purification. Sample solutions of Cu( II) -peptide complexes were prepared by dissolving an equimolar mixture of copper sulfate and peptide in $CO_2$-free distilled water.

### *Apparatus*

For electrochemical measurements a Fuso model 3 12 polarograph and a NF Electronic FG-121B function generator were used. A Fuso model

*Author to whom correspondence should be addressed.

**GHL = glycyl-L-histidyl-L-lysine; GHG = glycyl-L-histidylglycine; GH = glycyl-L-histidine; GGG = triglycine; GGH = glycyl-L-histidine.

0020-1693/91/$3.50

922 drop interval timer was attached to the polarograph for the measurement of drop time.

A Horiba F-8AT pH meter equipped with a No. 6327 high precision combination electrode was used for potentiometric titration.

*Potentiometric titrations*

Titrations were carried out on a 2 mM (mM = $10^{-3}$ mol $dm^{-3}$) peptide aqueous solutions for the determination of acid dissociation constants, and on 1 mM peptide aqueous solutions containing an equimolar amount of $CuSO_4$ for the determination of complex formation constants. Appropriate amounts of HCl and 0.1 M KC1 were added to the peptide solutions to adjust the initial pH and ionic strength, respectively. The peptide solutions were titrated with 0.1 M KOH at 25 + 0.1 "C. The measurements were carried out in nitrogen atmosphere to avoid contamination by $CO_2$. For each titration, 60-80 points were measured.

The calculations of the acid dissociation constants and the complex formation constants were carried out with the aid of computer calculation programs PKAS [14] and SCOGS2 [15], respectively.

*Electrochemical measurements*

All measurements were carried out in aqueous solution containing 0.1 M sodium perchlorate ($NaClO_4$) unless otherwise stated. Britton–Robinson buffer was used for pH adjustment. The working electrode used was a dropping mercury electrode (DME) for polarography and a Metrohm EA-209 hanging mercury drop electrode (HMDE) for voltammetric and electroplating measurements. A platinum plate and a saturated calomel electrode (SCE) were used as the counter and reference electrodes, respectively. All potential values are reported versus the SCE reference electrode. Dissolved oxygen was removed by bubbling the solution with pure nitrogen gas. All measurements were carried out at 25 ± 0.5 "C.

The electroplating experimental procedure consisted of three steps: (i) a HMDE was immersed in the appropriate copper solution and the potential was held constant at -0.6 V in order to reduce the copper species, although several potential scans were performed to monitor the surface state of the electrode (pretreatment step); (ii) the electrode was gently washed with distilled water and allowed to air dry; (iii) the electrode was immersed in a test solution and cyclic voltammograms were recorded (voltammetric step). Copper sulfate or Cu( 11) – GHL solutions were used for the pretreatment step. The test solutions used for the voltammetric step were either GHL solution or the base solution which contains only buffer reagent.

In electrocapillary measurements, each drop interval of DME was recorded and averaged over 10 drops for each potential.

## Results and discussions

*Potentiometric titrations*

A general equilibrium scheme containing metal ion, M, proton, H, and ligand (mono-anionic form in the present case), L, can be written as

$$pM + qH + rL \longleftrightarrow M_p H_q L_r \quad (1)$$

where $p, q$ and $r$ denote the stoichiometric numbers of metal, proton and ligand, respectively [9]. The overall formation constants of complexes, $\beta_{pqr}$, are defined as

$$\beta_{pqr} = \frac{[M_p H_q L_r]}{[M]^p[H]^q[L]^r} \quad (2)$$

where brackets denote the concentration of each component in mol $dm^{-3}$.

Tables 1, 2 and 3 show the lists of log $\beta_{pqr}$ for Cu( II) –GHL, Cu( II) -GHG and Cu(II) – GH, respectively. A negative integer value of $q$ in the

TABLE 1. Log $\beta_{pqr}$ values for GHL and Cu(II)-GHL[a]

| p q r | Log $\beta_{pqr}$ present study | Log $\beta_{pqr}$ literature values | |
|---|---|---|---|
| | | Ref. 9 | Ref. 8 |
| 0 11 | 10.19(0.13)[b] | 10.01' | 10.44[d] |
| 0 21 | 17.90(0.11) | 17.66 | 18.37 |
| 0 31 | 24.37(0.01) | 23.99 | 24.90 |
| 0 41 | 27.26(0.01) | 26.51 | 27.81 |
| 1 11 | 18.91(0.11) | 19.00 | |
| 1 01 | 15.70(0.01) | 16.12 | 16.44 |
| O-1 1 | 6.39(0.03) | 7.01 | 7.48 |
| 1 - 2 1 | −4.61(0.03) | -3.01 | − 3.74 |

"In Tables 1 -3, the data cited from the literature are limited to results from potentiometric titrations and to cases where the metal-to-ligand ratio was 1: 1. [b]Values in parentheses denote the standard error. '37 °C, 0.1 M $NaNO_3$. [d]25 °C, 0.15 M NaCl.

TABLE 2. Log $\beta_{pqr}$ values for GHG and Cu(II) -GHG

| p q r | Log $\beta_{pqr}$ present study | Log $\beta_{pqr}$ literature values | |
|---|---|---|---|
| | | Ref. 4 | Ref. 16 |
| 0 11 | 8.02(0.01) | 8.17" | |
| 0 21 | 14.55(0.03) | 14.80 | |
| 0 31 | 17.67( 0.03) | 17.99 | |
| 1 01 | 9.38(0.03) | | 8.52[b] |
| 1 – 1 1 | 5.59(0.01) | | 5.32 |
| 1 - 2 1 | −3.86(0.02) | | -3.69 |

"21 °C. [b]37 "C, 0.15 M $KNO_3$.

TABLE 3. Log $\beta_{pqr}$ values for GH and Cu(II)–GH

| $p$ | $q$ | $r$ | Log $\beta_{pqr}$ present study | Log $\beta_{pqr}$ literature values | | |
|---|---|---|---|---|---|---|
| | | | | Ref. 4 | Ref. 16 | Ref. 17 |
| 0 | 1 | 1 | 8.36(0.04) | 8.33[a] | 7.97[b] | 8.195[c] |
| 0 | 2 | 1 | 15.20(0.01) | 15.18 | 14.55 | 14.946 |
| 0 | 3 | 1 | 17.89(0.01) | 17.93 | 17.24 | 17.406 |
| 0 | 1 | 1 | | | 12.25 | |
| 1 | 0 | 1 | 9.15(0.06) | | 8.68 | 9.144 |
| 1 | −1 | 1 | 4.79(0.02) | | 4.54 | 4.885 |
| 1 | −2 | 1 | −5.38(0.04) | | −4.94 | −1.840 |

[a]21 °C. [b]37 °C, 0.15 M $KNO_3$. [c]25 °C, 0.1 M $KNO_3$.

Tables refers to a peptide deprotonation state beyond the mono-anion. The values of log $\beta_{pqr}$ determined in this study are in good agreement with literature values. Figures 1 and 2 show the species distribution profiles of Cu(II)–GHL and Cu(II)–GHG, respectively, as a function of pH. Cu(II)–GH showed a similar distribution profile to Cu(II)–GHG, in which $ML_{-H}$ (subscript −H denotes the further deprotonated state from the mono-anionic form of peptide) was the major species across most of the pH range including the neutral region, while ML was the major species in the case of Cu(II)–GHL.

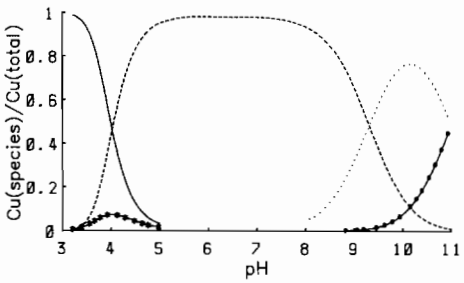


Fig. 1. Species distributions as a function of pH for the solution of $CuSO_4$ (0.999 mM) and GHL (0.980 mM). Notation of Figs. 1 and 2: —— free Cu(II), —•— MHL, --- ML, ··· $ML_{-H}$, —●— $ML_{-2H}$.

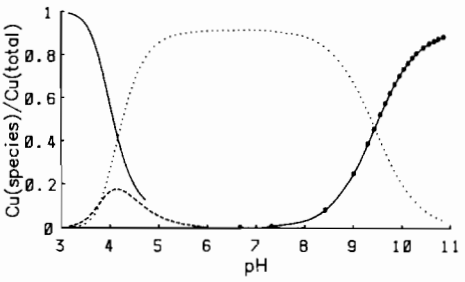


Fig. 2. Species distributions as a function of pH for the solution of $CuSO_4$ (0.999 mM) and GHG (0.914 mM).

As coordination sites of GHL to Cu(II), Freedman and coworkers proposed α-amino nitrogen, imidazole nitrogen and the nitrogen of the peptide bond between glycyl and histidyl residues [7, 18]. In contrast, Lau and Sarkar proposed the ε-amino nitrogen, the side chain of the lysyl residue, rather than the imidazole nitrogen by considering the significant difference between the $\beta_{101}$ values of Cu(II)–GHL and Cu(II)–GHG [8]. As pointed out by Rainer and Rode, however, these values cannot be compared with each other because GHL and GHG differ in the number of deprotonation sites [9]. In this study, a comparison of the distribution profiles in Figs. 1 and 2 indicates that the coordination sites of MLH and ML in Cu(II)–GHL are the same as those of ML and $ML_{-H}$ in Cu(II)–GHG and in Cu(II)–GH. This is reasonable if the ε-amino nitrogen of GHL is protonated at low pH and is not involved with a coordinate bond of MLH and of ML. The change in the major species in Fig. 1 from ML to $ML_{-H}$ at pH = 9 can then be attributed to deprotonation of the ε-amino nitrogen of the lysyl residue. The good agreement of the magnitudes of $\beta_{1\text{-}11}$ and $\beta_{1\text{-}21}$ for these three Cu(II)–peptide complexes supports the theory that the ε-amino residue of GHL was already deprotonated and hence the values of $\beta_{pqr}$ can be compared with those of the other two peptides.

Because the $ML_{-H}$ species of GH does not have an additional deprotonation site (the peptide bond between the second and third amino acid residue does not exist in GH), the change of $ML_{-H}$ to $ML_{-2H}$ is presumably caused by hydroxylation of the copper ion.

*Cyclic voltammetry*

As shown in Fig. 3, the cyclic voltammograms of Cu(II)–GHL, Cu(II)–GHG and Cu(II)–GH each exhibit one chemically irreversible reduction and one oxidation peak in 0.5 mM Cu(II)–peptide solutions at HMDE. Controlled-potential electrolysis at potentials more negative than that of the reduction peak gives rise to a color change

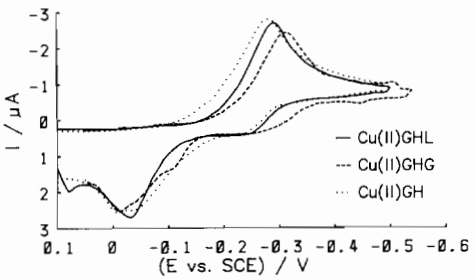


Fig. 3. Cyclic voltammograms of 0.5 mM Cu(II)–peptides in aqueous solutions of 0.1 M $NaClO_4$ at pH = 7.0. Working electrode was HMDE. Scan rate 60 mV/s.

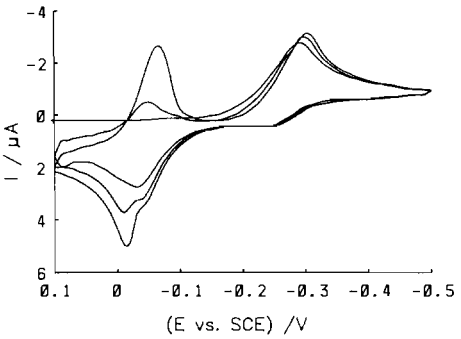


Fig. 4. Multi-cyclic voltammogram of 0.5 mM Cu(II)–GHL in aqueous solution of 0.1 M $NaClO_4$ at pH = 7.0. Working electrode was HMDE. Scan rate 60 mV/s.

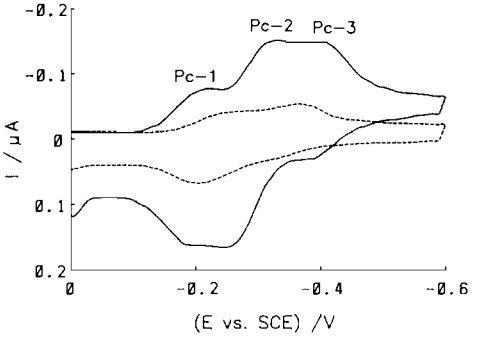


Fig. 5. Cyclic voltammograms of Cu(II)–GHL in aqueous solutions of 0.1 M $NaClO_4$ at pH = 9.0. Concentration of Cu(II)–GHL: --- 0.01 mM, —— 0.04 mM. Scan rate 30 mV/s.

of the mercury electrode surface to the bright color of copper metal, which indicates the reduction of Cu(II)–GHL to Cu(0) and the accumulation of copper metal at the mercury electrode. Thus in the cyclic voltammograms in Fig. 3, the cathodic peaks at *c.* −0.3 V are assigned to the reduction of the Cu(II)–peptide complexes, accompanied by loss of the coordinated peptide and adsorption of Cu(0). The anodic peaks are assigned to the oxidation of adsorbed Cu(0) to Cu(II). These peak assignments are supported by the multi-cyclic voltammogram of Cu(II)–GHL shown in Fig. 4, in which the redox peak current of the Cu(II)/Cu(0) couple (−0.07 V for cathodic and −0.02 V for anodic) increased with subsequent cycles of the potential scan.

The reduction peak of Cu(II)–GHL (−0.28 V at pH = 7.0) occurs at a potential between the reduction peaks of Cu(II)–GH (−0.27 V) and Cu(II)–GHL (−0.31 V). It is reasonable to consider that the similarity of the strengths of Cu(II)–peptide coordinate bonds is reflected in the similar values of these reduction potentials [19], although there are significant differences in the $\beta_{101}$ values of Cu(II)–GHL as compared to the other two complexes. Therefore, the larger $\beta_{101}$ value of Cu(II)–GHL does not necessarily mean that this complex is more stable than the other two complexes.

*Effects of the concentration change of Cu(II)–GHL*

As seen by comparing Figs. 3 and 5, the number of reduction peaks changes with the concentration of Cu(II)–GHL at pH > 5.0. The number of reduction peaks observed was 2, 3 and 1 for 0.01, 0.04 and 0.5 mM Cu(II)–GHL solutions, respectively (these peaks are labeled as Pc-1, Pc-2 and Pc-3 from less negative to more negative potentials). At pH < 4.0, the reduction peak of free Cu(II) ion was observed in addition to the above-mentioned peaks.

As shown in Fig. 6, the peak current of Pc-1 increased with increasing Cu(II)–GHL concentraiton until it reached a constant peak current at 0.2 mM. The peak labeled Pc-2 appeared at concentrations higher than 0.1 mM, and its peak current increased linearly with an increase in concentration of Cu(II)–GHL.

The peak current of Pc-1 increased linearly with scan rate, while that of Pc-2 showed a linear relationship with the square root of scan rate. This indicates that the adsorption of electroactive substances is involved in the electrode processes for Pc-1 and that the electrode reaction for Pc-2 is diffusion-controlled. The scan rate dependence of Pc-3 was similar to that of Pc-1, though accurate observation of Pc-3 was hindered by the overlap of Pc-2 with Pc-3.

Figure 7 shows the differential pulse voltammograms of Cu(II)–GHL. The width at half of the peak height, $\Delta E_{1/2}$, was about 60 mV for Pc-1; this value is somewhat larger than the theoretical

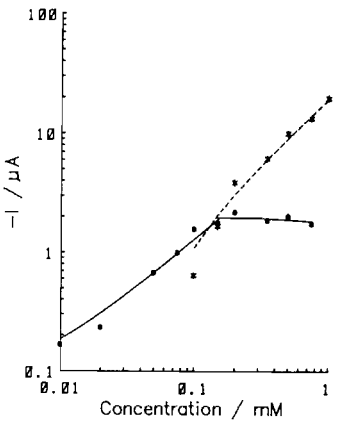


Fig. 6. Dependence of the peak current of Pc-1 (——) and Pc-2 (---) upon the concentration of Cu(II)–GHL by the differential pulse method at pH = 8.9. Scan rate 12 mV/s. Each point in figure indicates experimental values. The lines are least-squares fitted.

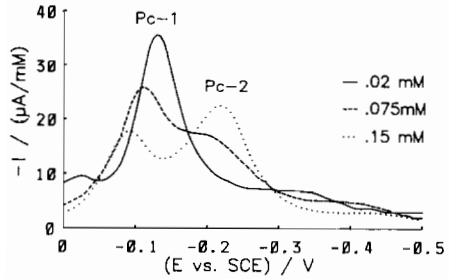


Fig. 7. Differential pulse voltammograms of Cu(II)–GHL at pH = 7.0. Concentration of Cu(II)–GHL: —— 0.02 mM, --- 0.075 mM, ··· 0.15 mM. Scan rate 1 mV/s, pulse amplitude 20 mV.

value of two-electron reduction (theoretical values are 90.4 and 45.2 mV for one- and two-electron reduction, respectively). As pointed out by Bard and Faulkner [19], however, the valuc of $\Delta E_{1/2}$ will be larger in the irreversible system compared to the reversible system, because the rising portion of an irreversible wave extends over a larger potential range. By taking into account this tendency, it is more probable that the Pc-1 corresponded to the two-electron reduction of Cu(II)–GHL rather than the one-electron reduction, even with the larger value of $\Delta E_{1/2}$. Therefore, the generation of Cu(I) as a reduction intermediate of Cu(II) complexes, suggested by some authors [11, 12], does not apply to the present system.

*Effects of pH change*

Figure 8 shows the dependence of the half-wave potentials of Pc-1 and Pc-2 on pH, as measured by polarography within the range of $4 < pH < 10$; the half-wave potential of both peaks shifted negative with increasing pH. The

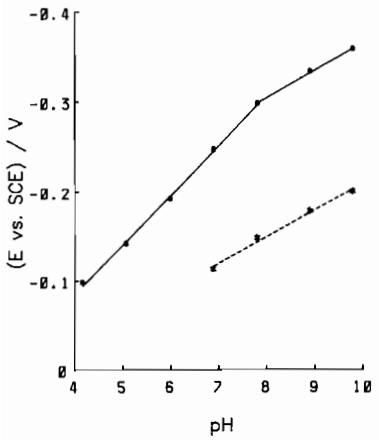


Fig. 8. Dependence of the polarographic half-wave potentials of Pc-1 (---) and Pc-2 (——) upon pH for 0.5 mM Cu(II)–GHL. Supporting electrolyte 0.1 M $NaClO_4$. Scan rate 12 mV/s.

pH dependence of the half-wave potential corresponding to Pc-2 showed an inflection point at pH = 7.5; the half-wave potential is shifted by 60 mV in the negative direction per unit increase of pH in the range of $pH < 7.5$, while it is only shifted by 30 mV at $pH > 7.5$.

The number of protons which participate in the electrode reaction can be estimated by the following relationship [20].

$$dE_p/dpH = -59.2q/n \quad (3)$$

where $E_p$, $n$ and $q$ represent the half-wave potential in mV, the number of electrons involved in the reduction process, and the number of protons which are added to the reduction product, respectively. In the case of the reduction of Cu(II)–GHL, the value of $q$ was estimated to be 2 and 1 for $pH < 7.5$ and $pH > 7.5$.

*Reaction mechanism of Cu(II)–GHL*

From the results of the potentiometric titrations, the coordination sites of GHL to Cu(0) can be assigned as the α-amino nitrogen, peptide bond between the glycyl and histidyl residues and the imidazole nitrogen. The voltammetric measurements show that the species contributing to the electrode reaction at $pH < 7.5$ is different from that at $pH > 7.5$. Dissociation of the metal–peptide bond was suggested by the results of multi-cyclic voltammetry. From these results, the reduction scheme of Cu(II)–GHL can be presented as follows

$$Cu(II)\text{–}H_pGHL_{-H}^{p+} + qH^+ + 2e^- \longrightarrow Cu(0)_{amal} + H_{p+q-1}GHL^{(p+q-2)} \quad (4)$$

where $Cu(0)_{amal}$, $H_p$, and subscript $-H$ denote the amalgamated copper metal, the number of titrable protons attached to GHL, and the deprotonated state of peptide bonds, respectively. The distribution profile of Cu(II)–GHL shows the ML form as a major species in the wide pH range, including in the neutral region (Fig. 1).

By taking into account the above results and the values of $q$, the following reaction schemes can be proposed for the pH regions above and below pH = 7.5:

(a) at $pH > 7.5$ (only ε-amino nitrogen of GHL is protonated)

$$Cu(II)\text{–}H_1GHL_{-H}^{+} + H^+ + 2e^- \longrightarrow Cu(0)_{amal} + H_1GHL \quad (5)$$

(b) at $pH < 7.5$ (α-amino nitrogen and ε-amino nitrogen of GHL are protonated)

$$Cu(II)\text{–}H_1GHL_{-H}^{+} + 2H^+ + 2e^- \longrightarrow Cu(0)_{amal} + H_2GHL^+ \quad (6)$$

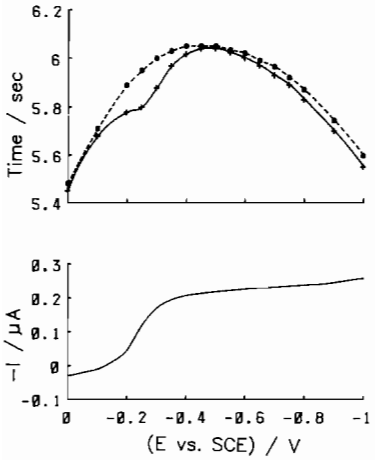


Fig. 9. Electrocapillary curve (upper) and trace of the polarogram (lower) in the solution of 0.1 mM Cu(II)–GHL and 0.1 M KCl. The electrocapillary curve was measured by counting the drop time of DME. The broken line in electrocapillary curve indicates the drop time of 0.1 M KCl base solution.

The assignments of these reaction species are in agreement with the distribution profiles of Cu(II)–GHL and GHL at pH > 6. From the results of potentiometric titration, however, the ML form of Cu(II)–GHL and the $LH_3$ form of GHL are suggested as the major species at pH < 6, which seems to conflict with the voltammetric results in the lower pH region. This issue can be resolved by considering the effect of electrostatic repulsion between the charged electrode surface and GHL. As shown in Fig. 9, the potential of Pc-2 was situated at the positive branch of the electrocapillary curve, indicating that the electrode surface has net positive charge in the potential region where the reduction proceeds. GHL also has a positive charge when doubly protonated. Therefore, the electric field near the electrode may prevent further protonation of doubly protonated GHL within the effective distance of electrode potential. The third protonation of GHL is attained only after the doubly protonated GHL has diffused away from the electrode-solution double-layer region. Hence, eqn. (6) still holds for the electrode reduction of Cu(II)–GHL in solutions of pH < 6.

*Electrocapillarity*

As expected from voltammetric measurements, the electrocapillary curve of Cu(II)–GHL solution shows adsorption of an electrode species in the potential range of −0.2 to −0.4 V. In contrast, the electrocapillary curve of GHL solution showed no evidence of adsorption (Fig. 9).

*Electroplating*

*(1) 0.1 mM $CuSO_4$ (pretreatment) ⟶ 0.1 mM GHL (voltammetry)*

After the mercury electrode was pretreated in $CuSO_4$ solution, the voltammograms in GHL solution showed redox peaks corresponding to Cu(II)–GHL, while no redox peak corresponding to free Cu(II) ion was observed as shown in Fig. 10. The peak currents of Cu(II)–GHL gradually decreased in subsequent cycles of the potential scan. These observations indicate that as the Cu(0) was oxidized to Cu(II), it reacted immediately with the free GHL in the solution and desorbed from the electrode surface at the potential range where $Cu(0)_{amal}$ was oxidized.

*(2) 0.1 mM Cu(II)–GHL (pretreatment) ⟶ base solution (voltammetry)*

The mercury electrode was pretreated in 0.1 mM Cu(II)–GHL solution. The reduction peaks of both Cu(II)–GHL and free Cu(II) ion were observed during the pretreatment step, and the latter peak increased with treatment time. Only the reduction peak of free Cu(II) ion was observed in the voltammetric step, and this peak decreased gradually with multiple cycles of potential scan (Fig. 11). These results indicate that upon reducing Cu(II)–GHL at the mercury electrode, GHL was not adsorbed to the electrode surface, and that only Cu(0) remained at the electrode surface as an amalgam. The results also indicate that, if free GHL was not contained in the test solution, a considerable amount of Cu(II) remained at the electrode surface, because the reduction peak of Cu(II) was observed during several cycles of the potential sweep.

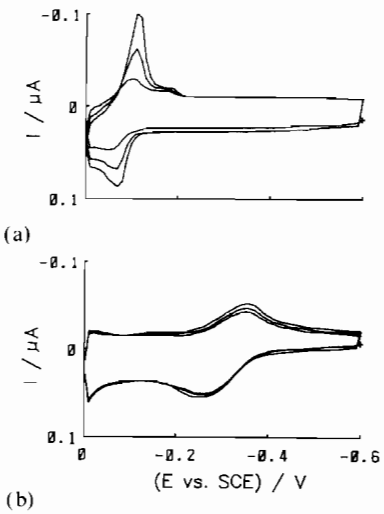


Fig. 10. Cyclic voltammograms of (a) 0.1 mM $CuSO_4$ during electroplating at −0.6 V (vs. SCE), and (b) 0.1 mM GHL after the electrode was treated by electroplating for 2 min. Scan rate 60 mV/s. pH = 8.9.

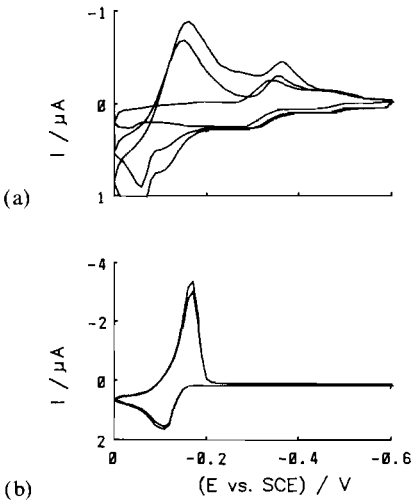


Fig. 11. Cyclic voltammograms of (a) 0.1 mM Cu(II)–GHL during electroplating at −0.6 V (vs. SCE), and (b) 0.1 M $NaClO_4$ base solution after the electrode was treated by electroplating for 2 min. Scan rate 60 mV/s. pH = 9.0.

*(3) 0.1 mM Cu(II)–GHL (pretreatment) ⟶ 0.1 mM GHL (voltammetry)*

After the mercury electrode was pretreated in 0.1 mM Cu(II)–GHL solution, the voltammograms in GHL solution showed both the reduction peaks of Cu(II)–GHL and of free Cu(II) ion, which is contrast to the results of the electroplating experiment (1). The peak corresponding to Cu(II) ion decreased rapidly with multiple cycles of the potential sweep, while the reduction peak current of Cu(II)–GHL remained constant as long as the reduction peak of free Cu(II) was observed. After the reduction peak of free Cu(II) diminished entirely, the peak of Cu(II)–GHL began to decrease gradually. These observations indicate that a constant amount of Cu(II)–GHL remained at the electrode surface until the free Cu(II) was entirely desorbed from the electrode surface in the voltammetric step.

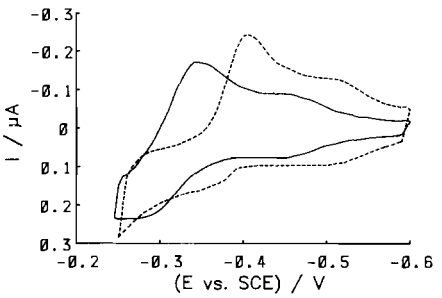


Fig. 12. Multi-cyclic voltammograms of GHL solution after the electrode was treated by electroplating in Cu(II)–GHL solution at −0.6 V (vs. SCE). Concentrations of GHL and Cu(II)–GHL: —— 0.1 mM, --- 0.5 mM. Supporting electrolyte 0.1 M $NaClO_4$, pH = 9.0, scan rate 60 mV/s.

The relations between the reduction peak current of Cu(II)–GHL and the concentration of GHL varied depending on the positive limit of the potential window. The Cu(II)–GHL peak current was proportional to the GHL concentration when the positive limit was set to 0.0 V. This concentration dependence was not obtained for solutions of 0.1 and 0.5 mM GHL when the positive limit was −0.25 V, in which case the peak currents were held at constant in the multiple cycles of potential sweep (Fig. 12).

*Adsorption mechanism of Cu(II)–GHL*

The results of electroplating experiment (3) seem in conflict with the results of electroplating experiment (1). This conflict, however, can be explained by considering the difference of the accumulation rate of Cu(0) in the pretreatment steps. In electroplating experiment (3), an excess amount of Cu(0) was accumulated on the mercury electrode in the pretreatment step as compared with electroplating experiment (1) (Figs. 10 and 11). Therefore, it is reasonable to consider that the desorption of Cu(II) was limited by the depletion of free GHL in the voltammetric step of electroplating experiment (3).

In electroplating experiment (2), the retardation of Cu(II) dissolution can be suggested to be caused by the formation of copper hydroxide and subsequent deposition on the electrode surface. The increase of the redox peak current of the Cu(II)/Cu(0) couple observed in Fig. 4 can also be explained by the same mechanism mentioned above, in which case free GHL diffused into the solution after the reduction of Cu(II)–GHL.

It is interesting to note that in electroplating experiment (3) the Cu(II)–GHL peak maintains a constant height when the positive limit of the potential window is set to −0.25 V, in which potential range the re-oxidation of $Cu(0)_{amal}$ does not occur and only the GHL-bound copper can be re-oxidized. These results indicate the adsorption of Cu(II)–GHL, because, if the Cu(II)–GHL was not adsorbed on the electrode surface, the reduction peak current should be decreased with the multiple cycles of potential scan. On the other hand, the possibility of adsorption of the reduction product was eliminated by the result of the electroplating experiment (2). From these results, it is concluded that Pc-1 shown in Fig. 5 is caused by the adsorption of Cu(II)–GHL itself and not by that of the reduction products of Cu(II)–GHL, which conclusion was supported by the electrocapillary measurement.

In the electroplating procedures, the accumulation of $Cu(0)_{amal}$ on the electrode brings about a variation in the electrochemical properties of the

electrode itself, which makes it difficult to assign the peaks to a particular species from the values of peak potential. The dependence of voltammetric behaviors on the potential window is of help in the assignment of these peaks. The fact that the peak currents are independent of the concentration, observed in the potential window of $-0.25$ to $-0.6$ V, clearly indicates that the peak is due to an adsorbed species.

Wopschall and Shain extensively studied the effects of the adsorption of electroactive species on voltammograms [21] and concluded that the pre-peak observed at less negative potential than that of the main peak of the voltammogram originates from the adsorption of the reduction product. However, the adsorption of Cu(II)–GHL may bring about a change in the coordination structure of Cu(II)–GHL, causing a shift of the redox potential of Cu(II)–GHL toward that of free Cu(II) ion. Wopschall's analysis is valid only in the case where adsorption does not give rise to a change of standard electrochemical potential of the electroactive species. Therefore, Wopschall's assignment cannot be applied to the present case.

From the adsorption behaviors of Cu(II)–GHL, it is concluded that the pre-peak (Pc-1) in the cyclic voltammograms is due to the reduction of adsorbed Cu(II)–GHL and that the change in the coordination structure of adsorbed Cu(II)–GHL is ascribed to the positive shift in peak potential of the adsorbed species. These peak assignments are supported by the electroplating results.

## References


1 S. J. Lau, T. P. A. Kruck and B. Sarkar, *J. Biol. Chem.*, *249* (1974) 5878.
2 S. J. Lau and B. Sarkar, *J. Chem. Soc. Dalton Trans.*, (1981) 491.
3 A. Yokoyama, H. Aiba and H. Tanaka, *Bull. Chem. Soc. Jpn.*, *47* (1974) 112.
4 H. Aiba, A. Yokoyama and H. Tanaka, *Bull. Chem. Soc. Jpn.*, *47* (1974) 1437.
5 L. Pickart and M. M. Thaler, *Nature New Biol.*, *234* (1973) 87.
6 L. Pickart, *In Vitro*, *17* (1981) 459.
7 J. H. Freedman, L. Pickart, B. Weistein, W. B. Mims and J. Peisach, *Biochemistry*, *21* (1982) 4540.
8 S. J. Lau and B. Sarkar, *Biochem. J.*, *199* (1981) 649.
9 M. J. A. Rainer and B. M. Rode, *Inorg. Chim. Acta*, *92* (1984) 1.
10 M. P. Youngblood and D. W. Margerum, *J. Coord. Chem.*, *11* (1981) 103.
11 P. S. Zacharias, T. Sreenivas and J. M. Elizabathe, *Polyhedron*, *5* (1986) 1383.
12 R. Bilewicz, *J. Electroanal. Chem.*, *267* (1989) 231.
13 M. Aihara, Y. Nakamura, Y. Nishida and K. Noda, *Inorg. Chim. Acta*, *124* (1986) 169.
14 A. E. Martell and R. J. Motekaitis, *Determination and Use of Stability Constants*, VCH, New York, 1989, p. 159.
15 D. D. Perrin and H. Stunzi, in D. J. Leggett (ed.), *Computational Methods for the Determination of Formation Constants*, Plenum, New York, 1985, p. 71.
16 R. P. Agarwal and D. D. Perrin, *J. Chem. Soc. Dalton Trans.*, (1975) 268.
17 G. Brookes and L. D. Pettit, *J. Chem. Soc. Dalton Trans.*, (1975) 2112.
18 A. L. Lehninger, *Biochemistry*, Worth, New York, 2nd edn., 1975, pp. 71–75.
19 A. J. Bard and L. R. Faulkner, *Electrochemical Method*, Wiley, New York, 1980, p. 164, 192–196.
20 L. Mites, *Polarographic Techniques*, Wiley, New York, 1965, 2nd edn., p. 217.
21 R. H. Wopschall and I. Shain, *Anal Chem.*, *39* (1967) 1514.